Springer

KSME

Journal of Mechanical Science and Technology 27 (3) (2013) 927~937
www.springerlink.com/content/1738-494x
DOI 10.1007/s12206-013-0104-0

Entropy analysis for nanofluid flow over a stretching sheet in the presence of heat generation/absorption and partial slip †

Aminreza Noghrehabadi*, Mohammad Reza Saffarian, Rashid Pourrajab and Mohammad Ghalambaz

Department of Mechanical Engineering, Shahid Chamran University of Ahvaz, Ahvaz, Iran

(Manuscript Received March 30, 2012; Revised July 31, 2012; Accepted September 6, 2012)

Abstract

The boundary layer heat transfer and entropy generation of a nanofluid over an isothermal linear stretching sheet with heat generation/absorption have been analyzed. In the nanofluid model, the development of nanoparticles concentration gradient due to slip mechanisms, the effects of Brownian motion and thermophoresis, is taken into account. The dependency of the local Nusselt number and entropy generation number on the non-dimensional parameters is numerically investigated. The results show that the increase of heat generation parameter, Brownian motion parameter, or thermophoresis parameter decreases the entropy generation number in the vicinity of the sheet.

Keywords: Nanofluid; Entropy generation; Similarity solution; Stretching sheet; Brownian motion; Thermophoresis

1. Introduction

The boundary layer flow and the heat transfer over a continuously moving surface are important types of flow and heat transfer that occur in several engineering processes. Heat-treated materials travel between a feed roll and a wind-up roll while they are subject to heat transfer with a fluid. Another example is the products manufactured by extrusion of plastic sheets [1]. These processes can be modeled as a stretching sheet subject to heat transfer. The stretching sheet phenomenon may occur in many other applications such as paper production, glass blowing, wire drawing, metal spinning, hot rolling, polymer engineering, cooling of metallic sheets and crystal growing [1, 2]. In these applications, the quality of the final product depends on the heat transfer rate between the stretching surface and the fluid during the cooling or heating process. Therefore, the choice of a suitable cooling/heating liquid is essential as it has a direct impact on the rate of heat transfer. Numerous techniques have been investigated to enhance thermal performance of heat transfer fluids. Porous materials can be used to enhance the heat transfer rate from stretching surfaces in the industrial applications [3, 4]. Another method is dispersing the nanoscale particles of highly thermal conductive materials like carbon, metal and metal oxides into heat transfer fluids to improve overall thermal conductivity. Nanofluid is described as a fluid in which the solid nanoparticles with the length scales of nanometers are suspended in a conventional heat transfer fluid. Sakiadis [5] was the first to study the boundary layer flow over a continuous stretching sheet. Many researchers have studied the different aspects of hydrodynamic boundary conditions including permeable stretching sheet, partial slip velocity on the sheet surface [6], and nonlinear velocity of stretching sheet. The appearance of global slip leads to an increase in the number of slipping atoms and consequently an increase in the slip length. Hayat et al. [7] analyzed the effect of the slip boundary condition on the magneto hydrodynamic flow and heat transfer over a stretching sheet. Makinde [8] analyzed the simultaneous effects of Navier slip and Newtonian heating on an unsteady hydromagnetic boundary layer stagnation point flow towards a flat plate. Makinde and Sibanda [9] studied the effect of chemical reaction on the boundary layer flow past a vertical stretching surface in the presence of internal heat generation. They found that the velocity and temperature profiles increase significantly as the heat generation parameter increases. Mehmood et al. [10] analytically analyzed the unsteady heat transfer and flow of an incompressible viscous fluid over a permeable isothermal stretching sheet. In certain applications such as those involving heat removal from nuclear fuel debris, underground disposal of radioactive waste material, and exothermic and/or endothermic chemical reactions, in the working fluid heat generation (source) or absorption (sink) effects are important. Kiwan and Ali [11] analyzed the flow and heat transfer characteristics of a fluid over a linearly stretching surface embedded in a saturated porous medium in the pres-

*Corresponding author. Tel.: +98 611 3330010, Fax.: +98 611 3336642
E-mail address: a.r.noyhrehabadi@gmail.com
† Recommended by Associate Editor Dongsik Kim

ence of internal heat generation or absorption near and far away of the slit. Alsaedi et al. [12] analyzed the effects of heat generation/absorption on stagnation point flow of nanofluid over a stretching surface.

Recently, Khan and Pop [13] analyzed the boundary-layer flow of a nanofluid past a stretching sheet using a model in which the Brownian motion and thermophoresis effect are taken into account. Noghrehabadi et al. [14] examined the effect of the partial slip boundary condition on the flow and thermal boundary layer of nanofluids over an isothermal stretching sheet. Das [6] did a case study for two types of nanofluids, Cu-water and Al_2O_3-water, to analyze the convective heat transfer performance of nanofluids over a permeable stretching surface in the presence of partial slip, thermal buoyancy and temperature-dependent internal heat generation or absorption.

The study of entropy generation has become an important aspect of modeling and optimizing application in the energy system to find their optimum design condition. The foundation of knowledge of entropy production goes back to Clausius and Kelvin's studies on the irreversible aspects of the second law of thermodynamics. Since then the theories based on these foundations have rapidly developed. However, the entropy production resulting from temperature differences has remained untreated by classical thermodynamics, which motivates many researchers to conduct analyses of fundamental and applied engineering problems based on second law of thermodynamics.

Entropy generation, which is common in all types of heat transfer processes, is associated with thermodynamic irreversibility. Different sources are responsible for generation of entropy like heat transfer across finite temperature gradient, characteristic of convective heat transfer, viscous effect and mass diffusion. Bejan [15, 16] focused on the different reasons behind entropy generation in applied thermal engineering. Generation of entropy destroys available work of a system. Therefore, it makes good engineering sense to focus on irreversibility of heat transfer and fluid flow processes to understand the function of entropy generation mechanism [15].

Many researchers have studied the entropy generation of thermal systems. Among them, Weigand and Birkefeld [17] analyzed entropy generation due to laminar flow over a flat plate. Makinde [18] performed a second law analysis for the hydromagnetic boundary layer flow and heat transfer over a stretching sheet in the presence of thermal radiation. Makinde considered variable viscosity as an inverse function of temperature difference and reported that the entropy generation number decreases as the Prandtl number, radiation parameter or viscosity variation parameter increases. In another study, Makinde [19] examined the inherent irreversibility in a gravity-driven thin liquid film along an inclined heated plate with convective cooling and found that viscous dissipation irreversibility is dominant at the inclined heated plate surface while the heat transfer irreversibility strongly is dominant at the liquid-free surface.

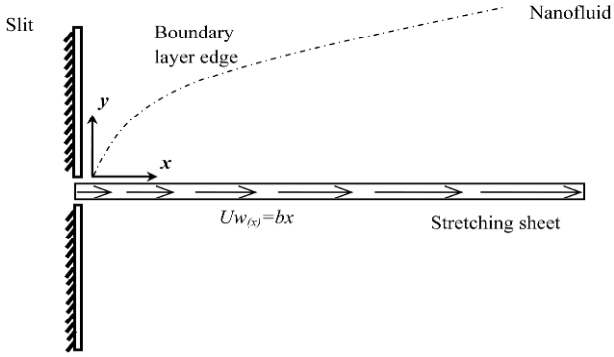

Fig. 1. Physical configuration and coordinate system of the problem.

Because of the novelty of nanofluids, only few works have been done to analyze the second law of thermodynamics in the area of nanofluid flow and heat transfer. Among them, Esmaeilpour and Abdollahzadeh [20] applied the second law to predict the nature of irreversibility in terms of entropy generation in the free convection flow and heat transfer of nanofluids inside an enclosure.

To the best of the authors' knowledge there is not any investigation to address the entropy generation of nanofluids using a model in which the dynamic effects of nanoparticles are taken into account. In the present study, the entropy generation, flow and thermal boundary layer over an isothermal stretching sheet are theoretically analyzed in the presence of the slip boundary condition and internal heat generation/absorption.

2. Mathematical formulation of the problem

Consider a two-dimensional incompressible and steady state viscous flow of a nanofluid over a continuously stretching surface. The velocity of surface is linear, which is taken as $U_W(x) = b.x$ where b is a constant, and x is the coordinate component measured along the stretching surface. The scheme of physical configuration has been depicted in Fig. 1. There are three distinct boundary layers, namely, hydrodynamic boundary layer (velocity), thermal boundary layer (temperature) and concentration boundary layer (nanoparticle volume fraction) over the sheet. However, in the Fig. 1 only a single boundary layer is plotted to avoid congestion. Here, the nanofluid flows at $y = 0$ where y is the coordinate measured normal to the stretching surface.

In the continuum modeling of fluidic transport, no-slip boundary condition is sometimes assumed, which means that the fluid velocity component is assumed to be zero relative to the solid boundary [21]. However, for nanofluids, a certain degree of tangential slip may be allowed [21, 22]. Considering the Navier condition, the velocity slip is assumed to be proportional to the local shear stress at the sheet surface [23].

The temperature and the nanoparticle fraction at the stretching surface are assumed to have constant values T_w and φ_w, respectively, while the ambient temperature and nanoparticle

fraction have constant values T_∞ and φ_∞, respectively. It is further assumed that the base (host) fluid and the suspended nanoparticles are in thermal equilibrium.

For nanofluids, by considering the dynamic effects of the nanoparticles and applying the boundary layer approximations the governing steady conservation of mass, momentum, thermal energy in the presence of heat generation or heat absorption in the Cartesian coordinate system of x and y are as follows [24, 25]:

$$\frac{\partial u}{\partial x}+\frac{\partial v}{\partial y}=0\,, \tag{1}$$

$$u\frac{\partial u}{\partial x}+v\frac{\partial u}{\partial y}=-\frac{1}{\rho_f}\frac{\partial p}{\partial x}+\nu\nabla^2 u \tag{2}$$

$$u\frac{\partial v}{\partial x}+v\frac{\partial v}{\partial y}=-\frac{1}{\rho_f}\frac{\partial p}{\partial y}+\nu\nabla^2 v \tag{3}$$

$$u\frac{\partial T}{\partial x}+v\frac{\partial T}{\partial y}=\alpha\nabla^2 T+\frac{Q_0}{\rho C_p}(T-T_\infty)+\tau\left\{\begin{matrix}D_B\nabla\varphi\cdot\nabla T+\\ \dfrac{D_T}{T_\infty}\nabla T\cdot\nabla T\end{matrix}\right\} \tag{4}$$

$$u\frac{\partial \phi}{\partial x}+v\frac{\partial \phi}{\partial y}=D_B\nabla^2\varphi+\left(\frac{D_T}{T_\infty}\right)\nabla^2 T \tag{5}$$

subject to the following boundary conditions at the sheet,

$$v=0,\ u=U_W(x)-U_S\,,\ T=T_W\,,\ \phi=\phi_W\,,\quad at\ y=0 \tag{6}$$

and the following boundary conditions at the far field

$$v=u=0\,,\ T=T_\infty\,,\ \phi=\phi_\infty\,,\quad y\to\infty\,. \tag{7}$$

Here, u and v are the velocity components along the x axis and y axis, respectively. T is the temperature, p is the fluid pressure, α is the thermal diffusivity, v is the kinematic viscosity, U_S is the velocity slip at the wall, Q_0 is the dimensional heat generation or absorption coefficient, D_B is the Brownian diffusion coefficient, and D_T is the thermophoresis diffusion coefficient. $\tau = (\rho c)_p /(\rho c)_f$ is the ratio of the effective heat capacity of the nanoparticle material and heat capacity of the fluid and ∇^2 is the Laplace operator in Cartesian coordinates. ρ and c are the density and specific heat capacity. The subscripts of p and f show the properties of nanoparticle and fluid, respectively.

Generally, the thermal diffusivity and diffusion coefficients are a function of the local volume fraction of nanofluids. In the present study, these properties are considered a function of quiescent volume fraction of nanofluid, φ_∞; hence, the effect of the local concentration due to the concentration gradient on the variation of these parameters has been neglected. As the nanofluids are dilute solutions, neglecting this effect on the variation of properties is a valid engineering assumption which has been applied by previous researchers [13, 26, 27]. Therefore, in the present study, the properties are evaluated for the nanoparticle volume fraction of quiescent nanofluid.

3. Nondimensionalization of the governing equations

To attain a similarity solution for Eqs. (1)-(5), the stream-function and dimensionless variables are introduced in the following form:

$$\psi=\sqrt{bv}\,x\,f(\eta),\qquad \eta=y\sqrt{b/v} \tag{8}$$

$$\psi=\sqrt{bv}\,x\,f(\eta),\qquad \eta=y\sqrt{b/v}\ . \tag{9}$$

The stream function ψ can be defined with $u = \partial\psi/\partial y$, $v = -\partial\psi/\partial x$, so that Eq. (1) is satisfied identically. The pressure outside the boundary layer in quiescent part of flow is constant, and the flow occurs only due to the stretching of the sheet; hence, the pressure gradient can be neglected. By applying the introduced similarity transforms Eqs. (8) and (9) on the remaining governing equations Eqs. (2)-(5) the following set of ordinary differential equations is obtained:

$$f'''+f\,f''-f'^2=0 \tag{10}$$

$$\frac{1}{pr}\theta''+f\,\theta'+\lambda\theta+Nb\,\beta'\theta'+Nt\,\theta'^2=0 \tag{11}$$

$$\beta''+\frac{Nt}{Nb}\theta''+Le\,f\,\beta'=0 \tag{12}$$

where primes denote differentiation with respect to η. The parameters of Pr, Le, Nb, Nt and λ are defined by:

$$\begin{aligned}&\mathrm{Pr}=\frac{\nu}{\alpha},Le=\frac{\nu}{D_B},Nb=\frac{(\rho c)_P D_B(\phi_W-\phi_\infty)}{(\rho c)_f\nu}\\ &Nt=\frac{(\rho c)_P D_T(T_f-T_\infty)}{(\rho c)_f\nu T_\infty},\lambda=\frac{Q_0}{\rho bC_p}\end{aligned} \tag{13}$$

where Pr, Le, Nb, Nt and λ denote the Prandtl number, Lewis number, Brownian motion parameter, thermophoresis parameter and the heat source ($\lambda > 0$) or sink ($\lambda < 0$) parameter, respectively.

Using the boundary layer approximations and introducing the Navier condition, the hydrodynamic boundary condition at the sheet surface can be written as:

$$u-U_w(x)=N\rho\nu\frac{\partial u}{\partial y}=U_s \tag{14}$$

where ρ is the nanofluid density and N is a slip constant. By applying the similarity transforms, the Eq. (14) is reduced to:

$$f'(0)-1=K\,f''(0) \tag{15}$$

where $K=N\rho(cv)^{1/2}$ is the non-dimensional slip factor. By performing introduced similarity transforms (i.e., Eqs. (8) and (9)) on the remaining boundary conditions (i.e., Eqs. (6) and

(7)), the transformed boundary conditions are obtained:

$$At\ \eta = 0:\ f = 0,\ f' = 1 + K f'',\ \theta = 1,\ \beta = 1 \tag{16}$$

$$At\ \eta \to \infty:\ f' = 0,\ \theta = 0,\ \beta = 0. \tag{17}$$

The quantity of practical interest in this study is the Nusselt number Nu_x:

$$Nu_x = \frac{x q_w}{k(T_w - T_\infty)} \tag{18}$$

where q_w is the wall heat flux. Applying the similarity variables yields:

$$\mathrm{Re}_x^{-1/2} Nu_x = -\theta'(0) \tag{19}$$

where $Re_x = U_{W(x)}\, x/v$ is the local Reynolds number based on the stretching velocity $U_{W(x)}$. Nield and Kuznestov [27] referred $\mathrm{Re}_x^{-1/2} Nu_x$ as the reduced Nusselt number $Nur = -\theta'(0)$.

Neglecting *Nb* and *Nt* reduces this problem to the classical problem of flow and heat transfer of a viscous fluid over a stretching surface with constant wall temperature [23, 28, 29]. In this case, the boundary value problem for β becomes ill-posed without physical meaning.

4. Entropy generation analysis

The local volumetric rate of entropy generation in the presence of finite temperature difference, viscous dissipation and mass diffusion is given by [30-33]:

$$S_G = \frac{k}{T_\infty^2}\left\{\left(\frac{\partial T}{\partial x}\right)^2 + \left(\frac{\partial T}{\partial y}\right)^2\right\} + \frac{\mu}{T_\infty}\left\{\left(\frac{\partial u}{\partial y}\right)^2\right\} + \left\{\frac{RD_B}{\phi_\infty}\left[\left(\frac{\partial \phi}{\partial x}\right)^2 + \left(\frac{\partial \phi}{\partial y}\right)^2\right] + \frac{RD_B}{T_\infty}\left[\left(\frac{\partial T}{\partial x}\right)\left(\frac{\partial \phi}{\partial x}\right) + \left(\frac{\partial T}{\partial y}\right)\left(\frac{\partial \phi}{\partial y}\right)\right]\right\}, \tag{20}$$

where (S_G) is the local volumetric entropy generation rate. Eq. (20) clearly shows contribution of entropy generation sources. The first term on the right-hand side of Eq. (20) is the entropy generation due to the heat transfer across a finite temperature difference (S_{th}), the second term is the local entropy generation due to viscous dissipation (S_{fr}), and the third term represents the diffusive irreversibility (S_{dif}).Therefore, the local entropy generation rate can be written as:

$$S_G = S_{th} + S_{fr} + S_{dif} \tag{21}$$

where the subscripts *th*, *fr* and *dif* are used to indicate the effect of thermal diffusion, viscous dissipation and concentration diffusion, respectively.

The dimensionless number for entropy generation rate (N_s) is defined by dividing the local volumetric entropy generation rate (S_G) to a characteristic entropy generation rate (S_{G0}). For the prescribed boundary condition, the characteristic entropy generation rate is:

$$s_{G0} = \frac{k(\Delta T)^2}{l^2 T_\infty^2}. \tag{22}$$

In the above equation, T_∞ is the absolute ambient temperature, ΔT is the temperature difference, and L is the characteristic length. Therefore, the entropy generation number is:

$$N_S = \frac{s_G}{s_{G0}}. \tag{23}$$

By applying the similarity transforms on the Eq. (23), the similarity equation of entropy generation is obtained as follows:

$$N_S = \mathrm{Re}_l\,\theta'^2(\eta) + \mathrm{Re}_l \frac{Br}{\Omega} f''^2(\eta) + \mathrm{Re}_l\,\varepsilon\left(\frac{\Sigma}{\Omega}\beta'(\eta)\right)^2 + \mathrm{Re}_l \frac{\varepsilon\Sigma}{\Omega}\theta'(\eta)\beta'(\eta). \tag{24}$$

In the above equation, N_s is the sum of three terms of irreversibility sources as $N_s = N_{th} + N_{fr} + N_{dif}$ where

$$N_{th} = \mathrm{Re}_l\,\theta'^2(\eta),\ N_{fr} = \mathrm{Re}_l \frac{Br}{\Omega} f''^2(\eta),\ N_{diff} = \mathrm{Re}_l\,\varepsilon\left(\frac{\Sigma}{\Omega}\beta'(\eta)\right)^2 + \mathrm{Re}_l \frac{\varepsilon\Sigma}{\Omega}\theta'(\eta)\beta'(\eta). \tag{25}$$

Br is the the Brinkman number, and Re_l is the Reynolds number based on the characteristic length. Ω is the dimensionless temperature difference and Σ is the dimensionless concentration difference. These parameters are given by the following relations:

$$\mathrm{Re}_l = \frac{u_l l}{\upsilon},\ Br = \frac{\mu u_w^2}{k(T_w - T_\infty)},\ \Omega = \frac{T_w - T_\infty}{T_\infty},\ \Sigma = \frac{\phi_w - \phi_\infty}{\phi_\infty},\ \varepsilon = \frac{RD_B\phi_\infty}{k}. \tag{26}$$

Here, the irreversibility distribution ratios can be defined as the irreversibility of each term to the total irreversibility. Therefore, the following non-dimensional parameters can be defined:

$$\gamma_{th} = \frac{N_{th}}{N_s},\ \gamma_{fr} = \frac{N_{fr}}{N_s},\ \gamma_{dif} = \frac{N_{dif}}{N_s}, \tag{27}$$

where γ_{th}, γ_{fr} and γ_{dif} denote the fraction of entropy generation due to thermal diffusion, viscous dissipation and concentration diffusion, respectively.

Table 1. Comparison of skin friction coefficient $-f''(0)$ for various values of slip factor K.

K	Present result	Sahoo and Do [28]	Wang [29]	Anderson [36]	Hayat et al. [7]
0.0	1.00000000	1.001154	1.0	1.0000	1.000000
1.0	0.43016066	0.428450	0.430	0.4302	0.430162
2.0	0.28398138	0.282893	0.284	0.2840	0.283981
5.0	0.14484373	0.144430	0.145	0.1448	0.144841
20	0.04379400	0.043748	0.0438	0.0438	0.043782

Table 2. Comparison of results for the reduced Nusselt number $-\theta'(0)$ when $Pr = Le = 10$ and $\lambda = K = 0$.

Nt	Nb	Present result	Khan and Pop [13]
0.1	0.1	0.95238	0.9524
0.2	0.1	0.69317	0.6932
0.3	0.1	0.52008	0.5201
0.1	0.2	0.50558	0.5056
0.1	0.3	0.25216	0.2522

5. Results and discussion

The set of ordinary differential Eqs. (10)-(12) subject to Eqs. (16) and (17) is solved numerically for various ranges of the Prandtl number, Lewis number, Brownian motion parameter, thermophoresis parameter, slip factor and heat source/sink parameter. Numerical results are obtained by using the Runge-Kutta-Fehlberg method [34, 35]. The most crucial factor of the solution is to choose the appropriate finite value of η_∞. Thus, to estimate the value of η_∞, it is increased from an initial value of 15 until the evaluated values of $f''(0)$, $\theta'(0)$ and $\beta'(0)$ differ only after the desired significant digit.

As a test of the accuracy of the solution, the values of $f''(0)$ in the case $Nb = Nt = 0$ are compared with the values reported by Wang [29], Sahoo and Do [28], Anderson [36] and Hayat et al. [7] for different values of the slip factor in Table 1. This table reveals that the numerical results obtained by the present algorithm are in very good agreement with the previous results. Table 2 shows the evaluated values of the reduced Nusselt number (Nur) for $Pr = 10$, $Le = 10$ in the case of the no slip condition and neglecting heat generation/absorption for several values of Brownian motion and thermophoresis parameter. The results of Table 2 in those cases are compared with Khan and Pop [13]. The comparison presented in Table 2 exhibits a fine agreement.

Values of the Prandtl number (Pr) and the Lewis number (Le) depend on the nature of the fluid. In gases $\alpha \approx \nu$ which leads to Pr and Le being of the order of unity. However, in most liquids $Pr > 1$ [37]; thus, heat diffusion is more efficient than mass diffusion, yielding a Lewis number which is greater than unity. The choice of the values for Nb and Nt was dictated by the fact that these values were used by Khan and Pop [13] and Makinde and Aziz [24] for the flow and heat transfer of nanofluids. In most cases of heat generation analyses for nanofluids, the parameter of λ considered in the range of -0.2 to 0.2 [6, 12, 25]. In the nanofluids, a limited range of temperature difference is applicable. High temperature differences may cause the evaporation of the base fluid which has not been considered in the present work. As the T_∞ is the absolute temperature, the value of Ω in most physical cases is on the order of magnitude of 10^{-1}. For the nanofluids, the magnitude of dynamic viscosity is of the scale of 10^{-3} and the term of $k(T_w-T_\infty)$ has the scale of 10^2. Therefore, Br and Br/Ω are small parameters. For the parameter of ε, the parameter of φ_∞ which shows the volume fraction of nanoparticles is of the order of 10^{-2}, and the magnitude of R/k is also of the order of 10^3. However, as Buongiorno [38] analyzed, D_B is a very small value. Consequently, the value of ε for nanofluids is also very small. The φ_w and φ_∞ are of the same order of magnitude. Thus, the parameter of Σ is also of the order of magnitude of 10.

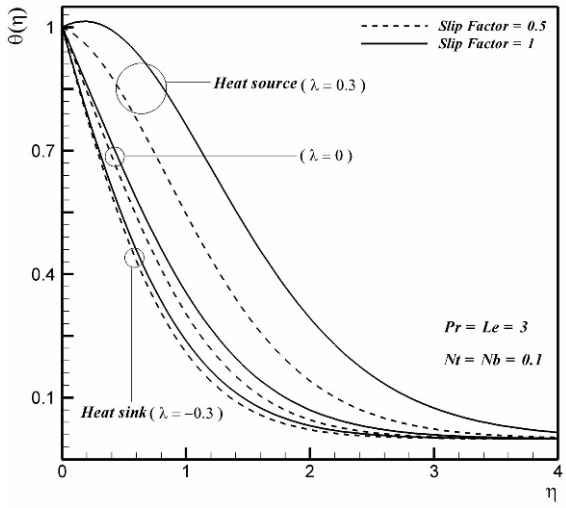

Fig. 2. Effect of heat source/sink parameter and slip factor on the dimensionless temperature profiles.

Fig. 2 shows the dimensionless temperature profiles $\theta(\eta)$ for selected values of the slip factor (K) and heat source/sink parameter (λ). In preparing this figure, Brownian motion, thermophoresis parameters, Lewis number and the Prandtl number were kept fixed. This figure illustrates that the nanofluid temperature in the vicinity of the sheet is high and decreases to zero at the edge of boundary layer, which satisfies the asymptotic far field boundary condition. The temperature in the thermal boundary layer rises as the slip factor or heat source/sink parameter increases. It is obvious that the increase of slip factor and heat source/sink parameter increases the magnitude of thermal boundary layer thickness. The increase of the heat source/sink parameter means the increase of the heat generated inside the boundary layer, which leads to higher temperature profiles. In the case of high values of heat generation ($\lambda = 0.3$) the maximum temperature occurs in the vicinity of the sheet, but not at the sheet. This observation is in good agreement with the physical insight of the problem. The temperature of fluid near the stretching sheet is high. There-

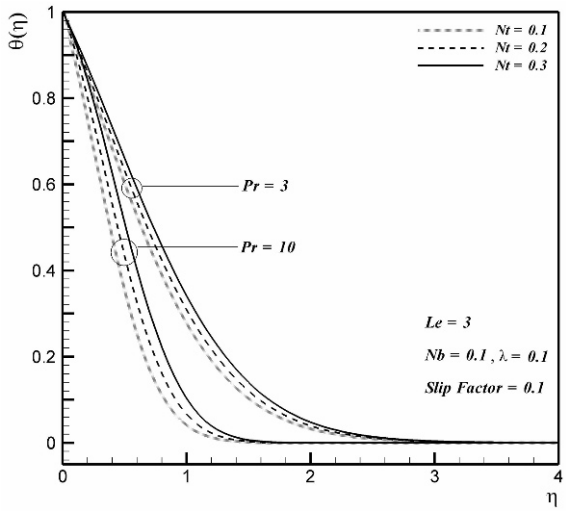

Fig. 3. Effect of Prandtl number and thermophoresis parameter on the dimensionless temperature profiles.

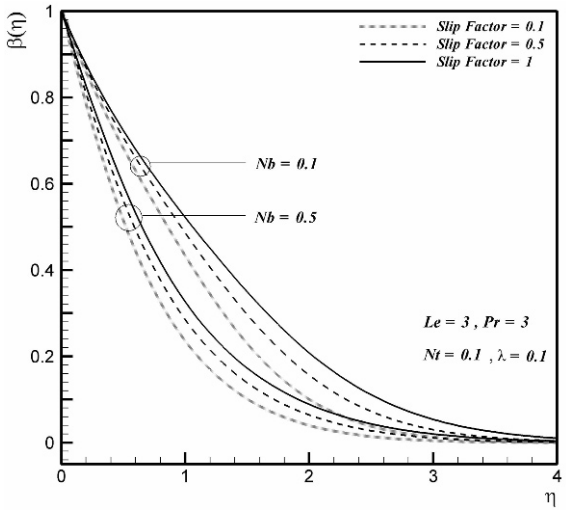

Fig. 4. Effect of Brownian parameter and slip factor on concentration distribution.

fore, addition of external heat which is generated in the boundary layer increases the fluid temperature to values higher than the temperature of stretching sheet. The presence of heat generation has the tendency to increase the fluid temperature. When heat absorption exists, the fluid temperature decreases, and the thermal boundary layer thickness becomes thinner. The movement of the flow in the boundary layer is because of the motion of the stretching sheet. Therefore, the increase of the slip factor decreases the effect of sheet motion on the boundary layer, and consequently, the flow tends to slow down. Thus, as the slip factor increases, the rate of heat transfer between the sheet and nanofluid decreases, and the thickness of thermal boundary layer increases.

The effects of Prandtl number and thermophoresis parameter on the dimensionless temperature profiles are shown in Fig. 3. As the thermophoresis parameter increases or the Prandtl number decreases, the local temperature profiles in the boundary layer increase. For a constant value of viscosity, the decrease of thermal diffusivity increases the magnitude of Prandtl number. Therefore, increase of Prandtl number decreases the diffusion of heat in the boundary layer, and thus the temperature profiles are increased. Fig. 4 illustrates the effects of Brownian motion and slip factor K on the concentration profiles. This figure shows that as the Brownian motion parameter increases, the concentration profiles decreases. By the increase of the Brownian motion parameter, the thickness of the concentration boundary layer is decreased. As the slip factor increases, the effect of stretching sheet on the boundary layer increases. Therefore, by the increase of the slip factor the concentration tends to rise in the vicinity of stretching sheet. However, far from the sheet, the slip factor does not have a significant effect on the thickness of the boundary layer.

As mentioned, the entropy generation number is the sum of three types of entropy sources: thermal diffusion, viscous dissipation and concentration diffusion. The contribution of each

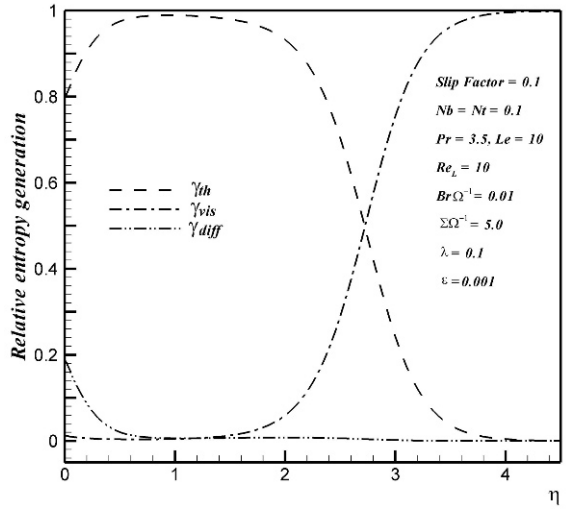

Fig. 5. Variations of relative entropy generation for each type of entropy generation source.

source of entropy in the boundary layer is depicted in Fig. 5. This figure reveals that near the sheet, the thermal diffusion is the dominant source of entropy generation. However, close to the sheet, which the velocity gradients are comparatively high, the entropy generation due to viscous dissipation also is comparatively significant. Near the boundary edge, which the temperature gradients are low, the local entropy generation due to viscous dissipation is the dominant source of entropy generation. It is worth noticing that near the boundary edge the total number of entropy generation is very small. Therefore, however, the entropy generation due to the viscous dissipation is dominant, but its magnitude is very low. The entropy generation due to concentration diffusion in the entire of boundary layer is slight. Figs. 6-11 show the effect of non-dimensional parameters of Le, Pr, Nt, Nb, λ and K on the entropy generation number, respectively. These parameters can

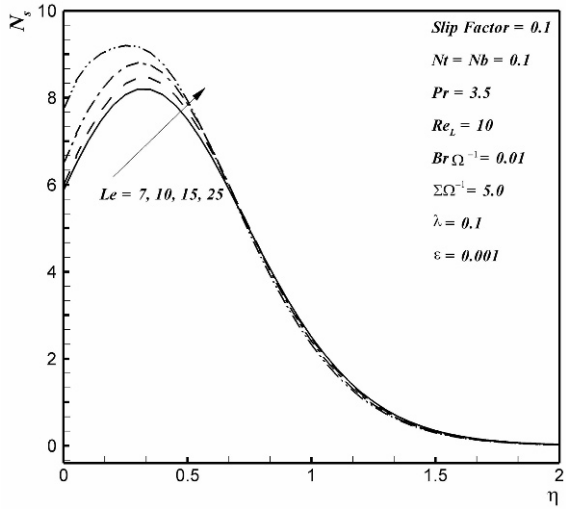

Fig. 6. Effect of Lewis number on the entropy generation number.

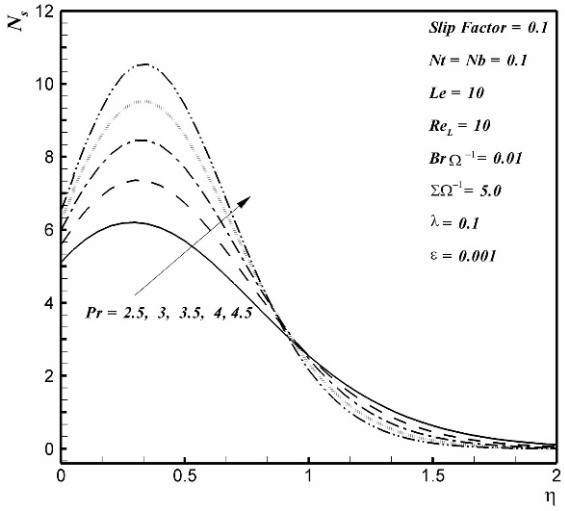

Fig. 7. Effect of Prandtl number on the entropy generation number.

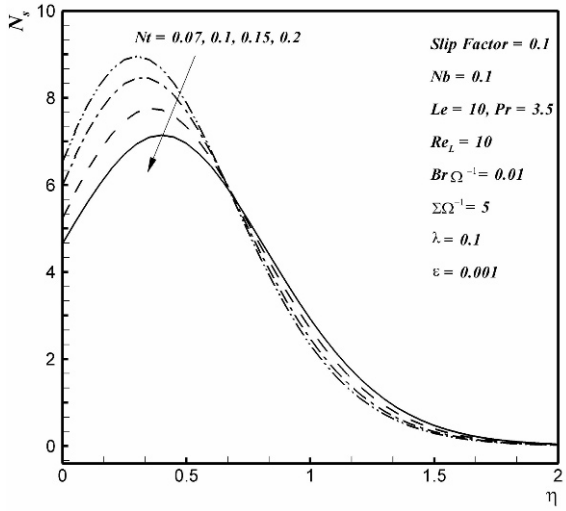

Fig. 8. Effect of thermophoresis parameter on the entropy generation number.

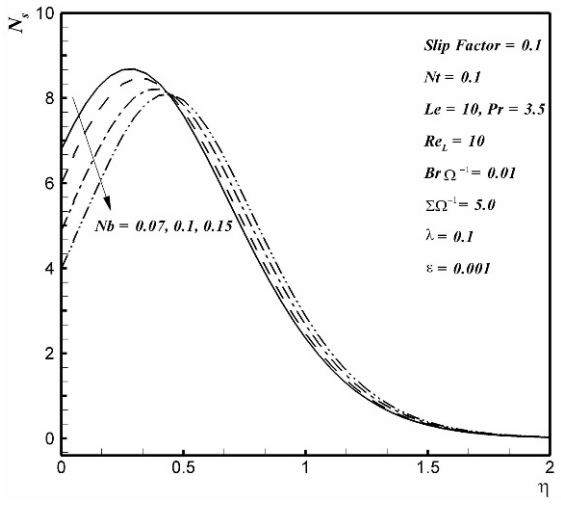

Fig. 9. Effect of Brownian parameter on the entropy generation number.

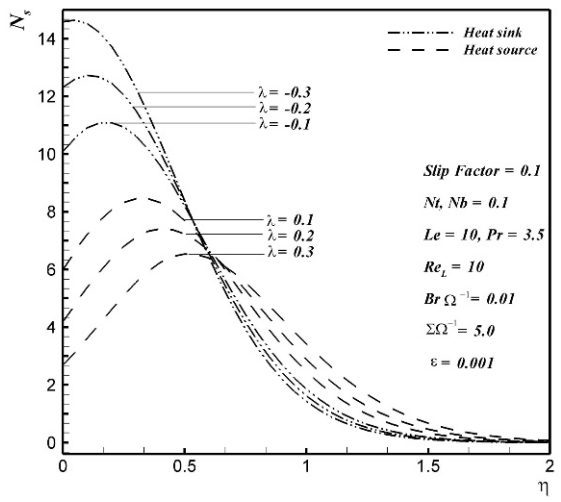

Fig. 10. Effect of heat source/heat sink parameter on the entropy generation number.

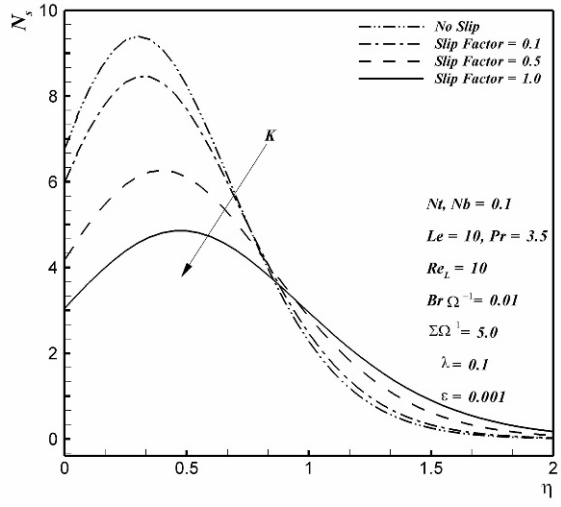

Fig. 11. Effect of slip factor on entropy generation number.

directly affect the flow, temperature, and concentration field inside the boundary layer, and consequently, they affect the entropy generation number. The increase of Lewis number affects the concentration, and consequently, the temperature profiles. The variation of Lewis number increases the entropy generation number at the vicinity of the sheet. However, far from the sheet it has not significant effect on the N_s (Fig. 6). Fig. 7 shows that as the Prandtl number increases, the entropy generation number increases gradually from the plate surface to its highest value in the vicinity of the plate and then decreases to the zero value of quiescent fluid. By contrast, in the places comparatively far from the sheet, the increase of Prandtl number decreases the entropy generation number. Figs. 8 and 9 demonstrate the effect of thermophoresis and Brownian motion on the entropy generation number, respectively. According to these figures, close to the sheet, as the thermophoresis parameter or Brownian motion parameter increases, the entropy generation number decreases. However, far from the sheet and inside the boundary layer, the increase of thermophoresis parameter or Brownian motion parameter increases the entropy generation number. Moreover, the entropy generation number is higher near the surface. This means that the surface acts as a strong source of irreversibility. Fig. 10 depicts the influence of the heat generation ($\lambda > 0$) and the heat absorption ($\lambda < 0$) parameter on entropy generation number. As the heat source/sink parameter λ increases, the entropy generation number decreases. Fig. 11 illustrates the effect of the slip factor on the entropy generation number. It is noticed that entropy generation increases as the slip factor decreases. The curves in the Figs. 6-11 have maximum value in the vicinity of the wall (not exactly on the wall). Based on the Fig. 2, the maximum values of the temperature were observed on the sheet or in the vicinity of the sheet and the minimum values of the temperature were observed on the edge of the boundary layer. Furthermore, moving from the surface to the edge of the boundary layer reduces the slop of the temperature curves. Therefore, the heat diffusion decreases by moving from the sheet to the edge of boundary layer. Hence, the maximum value of the heat diffusion also will be on the sheet or its vicinity. Now, by attention to the definition of the entropy generation ($dS'''_{gen} = \delta Q/T$), as moving from the boundary edge toward the sheet, the magnitude of temperature (T) and temperature slope (δQ) increase. Therefore, the denominator is trying to increase N_s, and the numerator is trying to decrease N_s. Hence, in a place on the sheet or in the vicinity of the sheet, the difference between the denominator and the numerator will have the least value, which will be the maximum entropy generation point where was observed in the Figs. 6-11.

Figs. 12-15 show the effect of Re_l, Br/Ω, Σ/Ω and ε on the entropy generation parameter. These parameters directly affect the entropy generation number. The augmentation of the Reynolds number increases the contribution of the entropy generation number due to fluid friction and heat transfer in the boundary layer. The increase of Reynolds number disturbs the

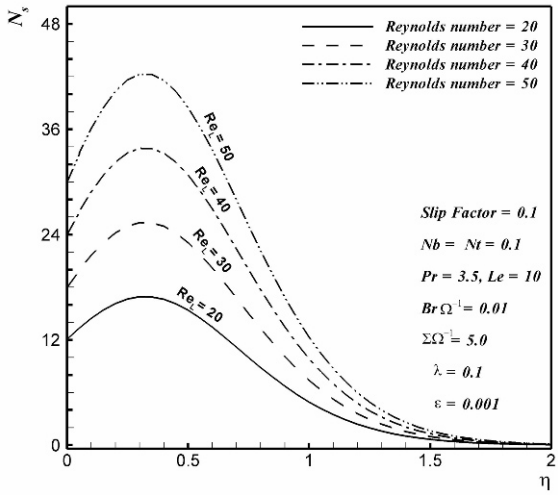

Fig. 12. Effect of Reynolds number on the entropy generation number.

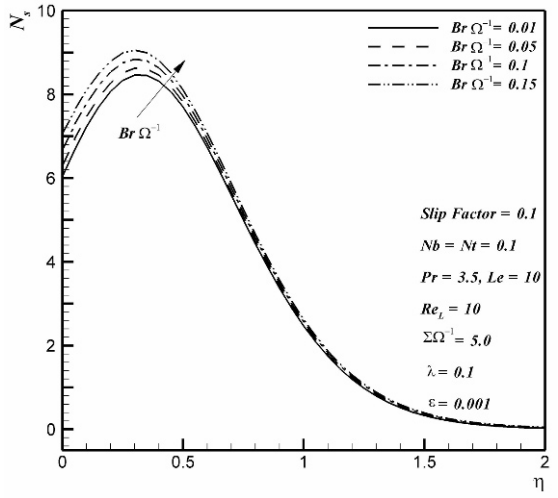

Fig. 13. Effect of dimensionless group parameter on entropy generation number.

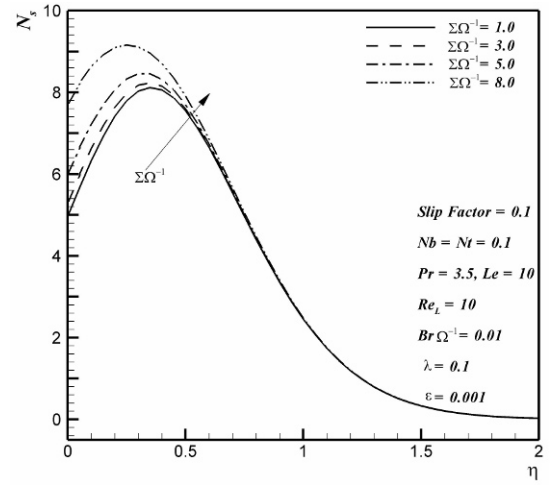

Fig. 14. Effect of the ratio of the dimensionless concentration difference to the dimensionless temperature difference on the entropy generation number.

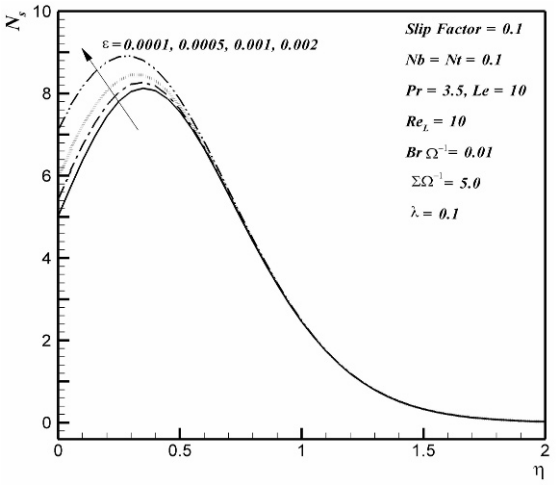

Fig. 15. Effect of the ε on the entropy generation number.

fluid, and then chaos appears in the fluid movement. The dimensionless group Br/Ω determines the relative importance of viscous effect. As the dimensionless group (Br/Ω) increases, the N_s increases. This augmentation is due to the fact that for higher values of the dimensionless group (Br/Ω), the entropy generation number due to the fluid friction is higher.

The parameter $\Sigma\Omega^{-1}$ is the ratio of the dimensionless concentration difference to the dimensionless temperature difference. For a given η, as this parameter increases, the entropy generation number increases. This augmentation is due to the contribution of the mass transfer to the entropy generation number. The parameter ε shows the contribution of the mass transfer to the entropy generation number. For a given η, as this parameter increases, the entropy generation number increases.

6. Conclusions

The effect of partial slip (i.e., Navier condition), heat generation as well as nanofluid parameters on the boundary layer flow, heat transfer and entropy generation of nanofluids past an isothermal stretching sheet is theoretically investigated. The boundary layer equations governing the flow, heat and nanoparticle are reduced to a set of nonlinear ordinary differential equations using the similarity transformations. The obtained differential equations are solved numerically for different combinations of nanofluid parameters. Effect of the slip factor (K), heat generation parameter (λ), Prandtl number (Pr) as well as the effect of nanofluid parameters including Lewis number (Le), Brownian motion parameter (Nb) and thermophoresis parameter (Nt) on the entropy generation are discussed. The obtained results can be summarized as follows:

The entropy generation due to thermal diffusion is the dominant source of entropy generation.

As λ and K increases the temperature and thermal boundary layer thickness increase while the Nusselt number and entropy generation number decrease.

As Prandtl number increases, the temperature decreases while the entropy generation at sheet nearby increases. Increasing the Prandtl number results in reduction of thermal boundary layer thickness and consequently the increase of Nusselt number and entropy generation number.

It is interesting that the increase of nanofluid parameters of Brownian motion and thermophoresis decreases the entropy generation at sheet nearby.

Increase of Le raises the temperature while it increases the entropy generation near the sheet.

As Re_l , $Br\Omega^{-1}$, Σ/Ω and ε increase, the entropy generation number increases.

In the present study, the nanofluid is considered as a dilute solution, and a simple boundary condition for the concentration of nanoparticles at the sheet surface has been adopted. Furthermore, the effect of the local volume fraction on the thermophysical properties has been neglected. Future studies can focus on the effect of this assumption on the heat transfer and entropy generation in the boundary layer.

Acknowledgment

The authors wish to express their very sincerely thanks to the reviewers for their valuable comments and suggestions. The authors are grateful to Shahid Chamran University of Ahvaz for its support through this paper.

Nomenclature

$(\rho c)f$	: Heat capacity of the fluid
$(\rho c)p$	: Effective heat capacity of the nanoparticle material
b	: Constant
Br	: Brinkman number
D_B	: Brownian diffusion coefficient
D_T	: Thermophoretic diffusion coefficient
k	: Thermal conductivity
K	: Dimensionless slip factor
Le	: Lewis number
N	: Slip constant
Nb	: Brownian motion parameter
Nt	: Thermophoresis parameter
N_s	: Entropy generation number
p	: Pressure
Pr	: Prandtl number
R	: Universal constant of gases Reynolds number
Re_l	: Reynolds number based on the characteristic length
Q	: Heat generation coefficient
S_G	: Local volumetric rate of entropy generation
S_{G0}	: Characteristic volumetric rate of entropy generation
T	: Fluid temperature
T_∞	: Ambient temperature
T_w	: Temperature at the stretching sheet
U_l	: Sheet velocity
u,v	: Velocity components along x- and y-axes
u_w	: Velocity of the stretching sheet

x,y : Cartesian coordinates (x-axis is aligned along the stretching surface and y-axis is normal to it)

Greek symbols

α : Thermal diffusivity
β : Dimensionless nanoparticle volume fraction
η : Similarity variable
ε : Constant parameter
θ : Dimensionless temperature
λ : Heat source/sink parameter
ρ_f : Fluid density
ρ_p : Nanoparticle mass density
φ : Nanoparticle volume fraction
φ_∞ : Ambient nanoparticle volume fraction
φ_w : Nanoparticle volume fraction at the stretching sheet
ψ : Stream function
Ω : Dimensionless temperature difference
Σ : Dimensionless concentration difference

References

[1] E. G. Fisher, *Extrusion of plastics,* Wiley, New York (1976).
[2] Z. Tadmor and I. Klein, *Engineering principles of plasticating extrusion,* Van Nostrand Reinhold, New York (1970).
[3] E. M. A. Elbashbeshy and M. A. A. Bazid, Heat transfer over an unsteady stretching surface*, Heat and Mass Transfer*, 41 (1) (2004) 1-4.
[4] A. Tamayol, K. Hooman and M. Bahrami, Thermal analysis of flow in a porous medium over a permeable stretching wall, *Transport in Porous Media*, 85 (2010) 661-676.
[5] B. C. Sakiadis, Boundary-layer behavior on continuous solid surface: I. Boundary-layer equations for two-dimensional and axisymmetric flow, *J AIChe*, 7 (1961) 26-33.
[6] K. Das, Slip flow and convective heat transfer of nanofluids over a permeable stretching surface, *Computers & Fluids*, 64 (15) (2012) 34-42.
[7] T. Hayat, M. Qasim and S. Mesloub, MHD flow and heat transfer over permeable stretching sheet with slip conditions, *Int. J. for Numerical Methods in Fluids*, 66 (8) (2011) 963-975.
[8] O. D. Makinde, Computational modelling of MHD unsteady flow and heat transfer toward a flat plate with Navier slip and Newtonian heating, *Braz. J. Chem. Eng,* 29 (1) (2012) 159-166.
[9] O. D. Makinde and P. Sibanda, Effects of chemical reaction on boundary layer flow past a vertical stretching surface in the presence of internal heat generation, *Int. J. of Numerical Methods for Heat & Fluid Flow*, 21 (6) (2011) 779-792.
[10] A. Mehmood, A. Ali and T. Shah, Heat transfer analysis of unsteady boundary layer flow by homotopy analysis method, *Communications in Nonlinear Science and Numerical Simulation*, 13 (5) (2008) 902-912.
[11] S. Kiwan and M. E. Ali, Near-Slit effects on the flow and heat transfer from a stretching plate in a porous medium, *Numerical Heat Transfer, Part A: Applications*, 54 (1) (2008) 93-108.
[12] A. Alsaedi, M. Awais and T. Hayat, Effects of heat generation/absorption on stagnation point flow of nanofluid over a surface with convective boundary conditions, *Commun Nonlinear Sci Numer Simulat*, 17 (11) (2012) 4210-4223.
[13] W. A. Khan and I. Pop, Boundary-layer flow of a nanofluid past a stretching sheet, *Int. J. of Heat and Mass Transfer*, 53 (11-12) (2010) 2477-2483.
[14] A. Noghrehabadi, R. Pourrajab and M. Ghalambaz, Effect of partial slip boundary condition on the flow and heat transfer of nanofluids past stretching sheet prescribed constant wall temperature, *Int. J. Thermal Sci.*, 54 (2012) 253-261.
[15] A. Bejan, Second-law analysis in heat transfer and thermal design, *Adv. Heat Transfer*, 15 (1982) 1-58.
[16] A. Bejan, *Entropy generation minimization,* CRC Press, Boca Raton, New York (1996).
[17] B. Weigand and A. Birkefeld, Similarity solutions of the entropy transport equation, *Int. J. Therm. Sci*, 48 (2009) 1863-1869.
[18] O. D. Makinde, Second law analysis for variable viscosity hydromagnetic boundary layer flow with thermal radiation and newtonian heating, *Entropy*, 13 (2011) 1446-1464.
[19] O. D. Makinde, Thermodynamic second law analysis for a gravity-driven variable viscosity liquid film along an inclined heated plate with convective cooling, *Journal of Mechanical Science and Technology*, 24 (4) (2010) 899-908.
[20] M. Esmaeilpour and M. Abdollahzadeh, Free convection and entropy generation of nanofluid inside an enclosure with different patterns of vertical wavy walls, *Int. J. Therm. Sci.*, 52 (2012) 127-136.
[21] M. Majumder, N. Chopra, R. Andrews and B. J. Hinds, Nanoscale hydrodynamics: Enhanced flow in carbon nanotubes, *Nature*, 438 (2005).
[22] R. A. Van Gorder, E. Sweet and K. Vajravelu, Nano boundary layers over stretching surfaces, *Commun. Nonlinear Sci. Numer. Simulat*, 15 (6) (2010) 1494-1500.
[23] C. Y. Wang, Analysis of viscous flow due to a stretching sheet with surface slip and suction, *Nonlinear Analysis: Real World Applications*, 10 (1) (2009) 375-380.
[24] O. D. Makinde and A. Aziz, Boundary layer flow of a nanofluid past a stretching sheet with a convective boundary condition, *Int. J. Therm. Sci.*, 50 (2011) 1326-32.
[25] M. A. A. Hamad and M. Ferdows, Similarity solution of boundary layer stagnation-point flow towards a heated porous stretching sheet saturated with a nanofluid with heat absorption/generation and suction/blowing: A Lie group analysis, *Commun. Nonlinear Sci. and Numer. Simulat*, 17 (1) (2012) 132-40.
[26] A. V. Kuznetsov and D. A. Nield, Natural convective boundary-layer flow of a nanofluid past a vertical plate, *Int. J. Therm. Sci.*, 49 (2010) 243-247.
[27] D. A. Nield and A. V. Kuznetsov, The Cheng-Minkowycz problem for natural convective boundary-layer flow in a

porous medium saturated by a nanofluid, *Int. J. Heat Mass Transfer*, 52 (25-26) (2009) 5792-5795.
[28] B. Sahoo and Y. Do, Effects of slip on sheet-driven flow and heat transfer of a third grade fluid past a stretching sheet, *Int. Commun. Heat and Mass Transfer*, 37 (8) (2010) 1064-1071.
[29] C. Y. Wang, Flow due to a stretching boundary with partial slip—an exact solution of the Navier-Stokes equations, *Chemical Engineering Science*, 57 (2002) 3745-3747.
[30] L. C. Woods, *Thermodynamics of fluid systems,* Oxford University Press, Oxford (1975).
[31] M. Mourad, A. Hassen, H. Nejib and B. B. Ammar, Second law analysis in convective heat and mass transfer, *Entropy*, 8 (2006) 1-17.
[32] H. F. Oztop and K. Al-Salem, A review on entropy generation in natural and mixed convection heat transfer for energy systems, *Renewable and Sustainable Energy Reviews*, 16 (1) (2012) 911-920.
[33] K. Ghachem, L. Kolsi, C. Mâatki, A. K. Hussein and M. N. Borjini, Numerical simulation of three-dimensional double diffusive free convection flow and irreversibility studies in a solar distiller, *Int. Comm. Heat Mass Transfer*, 39 (6) (2012) 869-876.
[34] E. Fehlberg, Low-order classical Runge-Kutta formulas with step size control and their application to some heat transfer problems*, in: Technical Report*, NASA (1969).
[35] E. Fehlberg, Klassische Runge-Kutta-Formeln vierter und niedrigerer Ordnung mit Schrittweiten-Kontrolle und ihre Anwendung auf Wärmeleitungsprobleme, *Computing Arch. Elektron. Rechnen*, 6 (1-2) (1970) 61-71.
[36] H. I. Andersson, Slip flow past a stretching surface, *Acta Mech*, 158 (1-2) (2002) 121-125.
[37] I. Pop and D. B. Ingham, *Convective heat transfer: mathematical and computational modelling of viscous fluids and porous media,* Elsevier Science & Technology Books, 2001.
[38] J. Buongiorno, Convective transport in nanofluids, *J. of Heat Transfer*, 128 (3) (2006) 240-250.

Aminreza Noghrehabadi is an assistant professor in the department of Mechanical Egineering at Shahid Chamran University of Ahvaz. His research interests are in nanofluid heat and mass transfer, NEMS actuators, and heat transfer in porous media.

Mohammad Reza Saffarian is an assistant professor in the department of Mechanical Engineering, Shahid Chamran University of Ahvaz. His research interests are in non-Newtonian fluid mechanics, settling tanks, gas tTurbines, and heating, ventilating, and air conditioning.

Rashid Pourrajab is a M.Sc. student in the department of mechanical engineering at Shahid Chamran University of Ahvaz. His research has been mainly focused on the development of new heat transfer enhancement fluid called nanofluids. He is working on modeling, production and experiments with nanofluids.

Mohammad Ghalambaz is currently Ph.D. student in the department of mechanical engineering at Shahid Chamran University of Ahvaz. His research interests are on the field of Nanofluid heat and mass transfer, NEMS actuators and Swarm optimization techniques.